Land cover changes the soil moisture response to rainfall on the Loess Plateau

Ge Fengchi[1], Mingxiang Xu[1], Chen Gong[2], Zuoyuan Zhang[2], and Qingyue Tan[1]

[1]Northwest Agriculture and Forestry University
[2]Chinese Academy of Sciences and Ministry of Water Resources Institute of Soil and Water Conservation

April 21, 2022

Abstract

Insight into the rainfall-soil moisture (SM) response to land cover is critical for soil hydrological process modeling and management. In this study, five typical land-cover types (forest, shrub, grass, crop, and bare land) and four rainfall patterns (heavy, intermediate, light, and continuous rains) were selected to assess the effects of SM response characteristics on the Loess Plateau of China. We monitored SM at five depths on each land-cover type at 1-h intervals over the growing season of 2019. The results showed that rainfall patterns and land-cover typestogether determined the SM response process and infiltration efficiency. A minimum accumulated rainfall amount of 5 mm was the threshold to trigger a 10-cm SM response. Rain events with higher intensity and smaller sum triggered a quick surface SM response, while larger amounts could percolate deeper and faster. Land-cover change significantly altered the rainfall-SM response dynamics and rainwater utilization efficiency after 20 years of ecological construction. Revegetation sites (mean values of forest, shrub, and grass) increased the soil wetting depth by 14.7%, shortened the SM response time by 27.3%, and accelerated the SM wetting front velocity by 67.2%, which promoted a 35.2% rainfall transformation rate (RTR) across the 1-m profile over all rainfall events (R_{1-13}). Moreover, planted forest showed the highest RTR of R_{1-13} and the maximal increase in soil water storage, which did not aggravate the soil water deficit across the 1-m profile over the growing season. Therefore, we present evidence that planted forests, instead of shrubs, may be beneficial for water conservation if precipitation is greater than 550 mm. The findings of this study prove the role of revegetation on rainwater infiltration capacity and efficiency and can help improve the management of afforestation in arid and semiarid regions.

Land cover changes the soil moisture response to rainfall on the Loess Plateau

Fengchi Ge [a], Mingxiang Xu [a, b, c, *], Chen Gong [b, c], Zuoyuan Zhang[d], Qingyue Tan [e],

[a] College of Forestry, Northwest A&F University, Yangling 712100, China

[b] Institute of Soil and Water Conservation, Northwest A&F University, Yangling 712100, China

[c] State Key Laboratory of Soil Erosion and Dryland Farming on the Loess Plateau, Institute of Soil and Water Conservation, Chinese Academy of Sciences and Ministry of Water Resources, Yangling 712100, China

[d] Institute of Soil and Water Conservation, Northwest A&F University, Yangling 712100, China

[e] College of Forestry, Northwest A&F University, Yangling 712100, China

Corresponding Author: Mingxiang Xu, Institute of Soil and Water Conservation, Northwest A&F University, Yangling 712100, China.

Email: xumx@nwsuaf.edu.cn

Abstract: Insight into the rainfall-soil moisture (SM) response to land cover is critical for soil hydrological process modeling and management. In this study, five typical land-cover types (forest, shrub, grass, crop, and bare land) and four rainfall patterns (heavy, intermediate, light, and continuous rains) were selected to assess the effects of SM response characteristics on the Loess Plateau of China. We monitored SM at five depths on each land-cover type at 1-h intervals over the growing season of 2019. The results showed that rainfall patterns and land-cover typestogether determined the SM response process and infiltration efficiency. A minimum accumulated rainfall amount of 5 mm was the threshold to trigger a 10-cm SM response. Rain events with higher intensity and smaller sum triggered a quick surface SM response, while larger amounts could percolate deeper and faster. Land-cover change significantly altered the rainfall-SM response dynamics and rainwater utilization efficiency after 20 years of ecological construction. Revegetation sites (mean values of forest, shrub, and grass) increased the soil wetting depth by 14.7%, shortened the SM response time by 27.3%, and accelerated the SM wetting front velocity by 67.2%, which promoted a 35.2% rainfall transformation rate (RTR) across the 1-m profile over all rainfall events ($R_{1\text{-}13}$). Moreover, planted forest showed the highest RTR of $R_{1\text{-}13}$and the maximal increase in soil water storage, which did not aggravate the soil water deficit across the 1-m profile over the growing season. Therefore, we present evidence that planted forests, instead of shrubs, may be beneficial for water conservation if precipitation is greater than 550 mm. The findings of this study prove the role of revegetation on rainwater infiltration capacity and efficiency and can help improve the management of afforestation in arid and semiarid regions.

Keywords: soil moisture response; land cover; rainfall; revegetation; soil water storage; Loess Plateau

1. INTRODUCTION

NOTE: What does the response dynamic of SM after rainfall look like under different land-cover types? What content and extent of the soil water percolation process are changed after revegetation? And which afforestation pattern can make the most effective use of rainfall to improve the water conservation function of vegetation? There is still no consensus and definite answer to these questions.

Climate drought and water deficiency are common problems in arid and semiarid regions around the world. Under the background of global warming (Williams et al., 2020), the dryland area will continue to expand (Feng and Fu, 2013; Lickley and Solomon, 2018), from 40% (Huang et al., 2016) of the global terrestrial ecosystem at present to 47% by the end of the 21st century (Koutroulis, 2019). Although water resources are scarce in arid and semiarid regions, soil losses in these regions are extremely serious (Fu et al., 2017; Mamedov and Levy, 2019; Wang et al., 2020), and this pattern is mainly related to the lack of vegetation coverage (Zhao et al., 2013), loose soil and easy erosion (Fu et al., 2017), as well as irregular but high-intensity rainfall in such areas (Mamedov and Levy, 2019). Therefore, drought and water and soil loss have become urgent contradictions in arid and semiarid regions of the world.

To solve this prominent problem, many countries and regions have adopted a close to natural solution, namely, planting trees (Zheng et al., 2016). Afforestation is considered to be the most economical and convenient way to restore the ecological environment and reduce water loss and soil erosion, so the practice has been widely recognized and accepted in the world (Bryan et al., 2018; Chirino et al., 2006; Liu et al., 2018; Wu et al., 2021). Since 1990, the area of artificial forest has increased by more than 105 million hectares, accounting for 7% of the global forest area (Birdsey., 2015). Revegetation has a significant impact on the hydrological process of an ecosystem by influencing evapotranspiration, water infiltration, runoff generation, soil erosion, and solute transportation (Ding et al., 2021; Su and Shangguan, 2019; Zhu et al., 2021), thus altering the terrestrial water recycling process.

The relationship between rainfall and SM has always been a core issue in the study of soil hydrological processes. In recent years, many studies have been conducted in this research field. For example, Rohit et al. (2011) assessed the impact of altered rainfall on soil-moisture dynamics in three annual grassland vegetation types. He et al. (2012) qualitatively described the influence of precipitation on the soil moisture of the rainy season in northwestern China's Qilian Mountains. Su et al. (2019) and Li et al. (2021b) used meta-analysis to illustrate that the relationship of rainfall and SM changed by vegetation construction

and afforestation led to a decline in SM on the Loess Plateau of China. Despite efforts to characterize the spatiotemporal variations in SM related to rainfall, but SM dynamics and infiltration processes cannot be determined after precipitation. In subsequent studies, Pan et al. (2019), He et al. (2020) and Mayerhofer et al. (2017) analyzed soil water infiltration, redistribution and runoff through laboratory or field experiments using simulated rainfall. Many studies have adopted continuous monitoring equipment to analyze SM dynamics after rainfall under different vegetation patterns but have reached different conclusions (Jin et al., 2018; Wang et al., 2012; Wang et al., 2013; Yu et al., 2015). For instance, Wang et al. (2013) suggested that the SM response to rainfall leads to the smallest accumulated infiltration and largest surface runoff occurring in grasslands. Jin et al. (2018) showed that forestland has a faster SM response time and deeper response depth than grassland but the smallest soil water storage. What does the response dynamic of SM after rainfall look like under different land-cover types? What content and extent of the soil water percolation process are changed after revegetation? And which afforestation pattern can make the most effective use of rainfall to improve the water conservation function of vegetation? There is still no consensus and definite answer to these questions.

As a typical arid and semiarid region in the world, the Chinese Loess Plateau (CLP) has suffered extremely serious soil erosion and water and soil loss for a long time (Chen et al., 2007b; Fu et al., 2017). To protect soil and water and curb ecological deterioration, the Chinese government implemented the 'Grain For Green' project at the end of the 20th century. Vegetation reconstruction significantly changed the land-cover type and vegetation structure, reshaped the mutual-feeding relationship and cycling process between the soil-vegetation-atmosphere continuum (SPAC) (Deng and Shangguan, 2017; Jia and Shao, 2014), and fundamentally contained water and soil loss and restored the ecological environment on the CLP (Fu et al., 2017). For instance, Zhao et al. (2017) and Fu et al. (2017) found that 20 years of revegetation reduced the runoff and sediment load of the Yellow River by 24.8% and 57%, respectively, which controlled soil erosion to a great extent. Moreover, many studies have confirmed that the conversion of farmland to trees or grasses enhances vegetation coverage and rainfall interception (Liu et al., 2020; Murray, 2014), improves soil texture (Li et al., 2006), and increases soil porosity, thus greatly promoting rainfall infiltration and soil water storage (Kijowska-Strugala et al., 2018; Sun et al., 2018). However, artificial vegetation consumes more soil water due to the larger evapotranspiration (Jia et al., 2017), which intensifies soil desiccation and even forms a dry soil layer (Wu et al., 2021), thus limiting plant growth and resulting in advanced senescence and degradation of artificial vegetation, such as the 'little old man tree' (Wang et al., 2010b). Consequently, the soil water deficit is one of the most important problems affecting the survival and sustainability of artificial afforestation (Li et al., 2021a). Improving the conversion efficiency of rainfall is a critical path to solving the soil water deficit problem. Therefore, it is particularly important to study the rainfall-soil moisture (SM) response process and its effect on rainwater transformation and utilization.

Based on the extensive existence of artificial vegetation and the need for understand soil water infiltration processes, this paper aimed to reveal the rainfall-SM response process and mechanism, and evaluate the effect of soil water infiltration and replenishment by different rainfall or vegetation land-cover types to clarified the optimal revegetation type on the semiarid region. To do this, we monitored the 1-h SM at five depths down to the 1 m depth (10, 30, 50, 70, and 100 cm) in typical land covers (forest, shrub, grass, crop, and bare land) over the growing season of 2019. We hypothesized that 20 years of revegetation has changed soil water replenishment patterns, promoted rainwater use efficiency and enhanced soil water storage in the growing season. The results of this study are expected to shed insight into profile soil water infiltration processes related to rainfall after vegetation restoration on the CLP and to provide design and optimization solutions for vegetation restoration in similar areas of arid and semiarid regions around the world.

2. MATERIALS AND METHODS

2.1 Study area

The study area is located in the Zhifanggou watershed (36°48' N, 109°15' E) in the loess hilly and gully region of northern Shaanxi Province, China (Fig. 1). This area belongs to a typical forest-grass zone with complex terrain, ravine and crisscross, and an elevation ranging from 997~1731 m. The region is mainly affected by the

semiarid continental climate in the warm temperate zone, with an average annual temperature of 8.8 and an annual rainfall of 500-600 mm. The natural vegetation of the area has been almost completely destroyed, and the restored plantations are composed of *Robinia pseudoacacia* ,*Populus simonyi* , *Caragana* korshinskii, and *Hippophae rhamnoides* . The abandoned slope is mainly composed of herbs at different stages of succession, such as *Artemisia gmelinii* ,*Artemisia Giraldi* , *Stipa bungeana* , and *Bothriochloa ischaemum* . The soil type is loessal soil, of which silt accounts for over 64%. In this area, the soil is loose with poor soil resistance, which leads to serious soil and water erosion.

In the watershed, typical land cover (forest, shrub, grass, crop, and bare land) was selected (Table 1). The same slope gradient site was chosen as the experimental plot (22deg~25deg), which was a 5x20 m standard experimental plot. In the forest plot, the major tree species was *Robinia pseudoacacia* . Many herbaceous plants grow here, such as *Stipa bungeana* , *Setaria viridis* , and*Leymus secalinus* . In the shrub plot, the main planted species was*Caragana korshinskii* , with many undergrowth vegetation types, such as *Artemisia gmelinii* , *Bothriochloa ischaemum* , and*Heteropappus altaicus* . In the grass plot, the dominant grass species were *Lespedeza daurica* , *Bothriochloa ischaemum* ,*Stipa bungeana* , *Artemisia gmelinii* , and*Leymus secalinus* . In the crop plot, the major crop species was*Syringa oblata* . The bare land plot did not have any plant growth and was weeded once a month.

2.2 Methods

2.2.1 Soil moisture monitoring

SM monitor has been established in typical land-cover sites since June 2018. At each site, an array of SM probes (EC-5 probes with a precision of +-0.1 vol. %; The METER Group, Inc., Pullman, Washington) was installed horizontally at five depths below the soil surface. According to previous studies, the SM response depth is limited to the 1-m profile of each land-cover type after the rainy season (Tang et al., 2018; Wang et al., 2013; Yu et al., 2015). Thus, we installed an SM monitoring probe in the 0-1-m profile (10, 30, 50, 70, and 100 cm) to investigate SM infiltration and the response process affected by rainfall. Meanwhile, this paper set the 10-cm soil layer as the shallowest monitoring depth to reveal the difference in surface SM response time and soil permeability after precipitation as a result of revegetation (Jin et al., 2018; Lee et al., 2017; Liu et al., 2020).

After installation, the pit was carefully refilled with original soil material and compacted to the original bulk density layer by layer to avoid perturbation as much as possible. SM was measured every h and stored in EM50 dataloggers (The METER Group, Inc., USA). The 1-h SM data from May 1 to October 31 in the growing season were used to explore the SM dynamics after rainfall.

2.2.2 Identification of rainfall process and soil wetting event

An automatic weather station was set up at the bare land uphill slope site. Rainfall was recorded every minute by a tipping bucket rain gauge (0.2 mm/tip; Jiangsu Naiwch Corporation Inc., China). The definition of a new rainfall process was when the 1-h rainfall amount was larger than 0.4 mm (surpassing the threshold of instrument noise) and recorded after the period without any rainfall record exceeding 48 h. We defined the end of the process when the rainfall amount was less than 0.2 mm for 48 h (i.e., the level of instrument noise). Within the rainfall process, we defined the timing of a rainfall record with an interval of more than 24 h from the previous rainfall record as the initiation of an individual rainfall event.

The concept of a soil wetting event was adopted, in which a significant increase in SM as the result of rainfall infiltration into the soil can be observed (Lozano-Parra et al., 2015; McMillan and Srinivasan, 2015). For all the probes, we defined the start time of the soil wetting event if the increase in accumulated SM was >0.2 vol.% greater than the initial SM (Hardie et al., 2013; Lin and Zhou, 2008). In our study, we found that SM was subject to soil temperature fluctuation that might cause a decrease at a rate of 0.1 vol.% per h during the daytime. An SM increment of 0.2 vol.% was selected to exceed the device noise (0.1 vol.% for the EC-5 SM probes) (Rosenbaum et al., 2010). Furthermore, we used the time without an increase in SM at 6 h as the end time of the soil wetting event process.

4

2.2.3 Soil moisture response to rainfall process

The SM response lag time (RT , h) was evaluated to characterize the temporal delay of the soil wetting process with depth. It is calculated as follows:

$RT = ST_i - ST_0$ (1)

where ST_i and ST_0 represent the SM response time at layer i (layer1: 0-10 cm, layer2: 10-30 cm, layer3: 30-50 cm, layer4: 50-70 cm, layer5: 70-100 cm) and rainfall time, respectively. According to this case, we recorded the accumulated rainfall amount (ARA , mm) that could trigger SM increases in different soil layers:

$ARA = \sum_{t=ST_0}^{ST_i}$ R (2)

where R represent the and real-time rainfall (mm), respectively.

Definition of the wetting front velocity (WFV , cm/h) at different soil depths used to describe the SM wetting dynamics after rainfall:

$WFV_{ij} = SWD_{ij} / RT_{ij}$ (3)

where SWD_{ij} and RT_{ij} are the soil wetting depth (cm) and the response time (h) at layer i in the jth soil wetting process, respectively.

2.2.4 Soil water storage variation in the rainfall process and growing season

In our study, we defined the absolute increase in SM (AIM , vol.%) at each measurement location as follows:

$AIM = SM_e - SM_s$ (4)

where SM_e (vol.%) and SM_s (vol.%) are the SMs at the end time of the soil wetting process and at the start time of rainfall, respectively. Additionally, we calculated the soil water storage variation at the 100 cm soil depth (SWS_{0-1m} , mm) after each rainfall process:

$SWS_{0-1m} = \sum_{i=1}^{5} AIM_i \times D_i \times 10$ (5)

where AIM_i represents the absolute increase in SM at layer i. D_i is the thickness of each depth interval. Then, the rainfall transformation rate (RTR , %) was calculated as follows:

$RTR = SWS_{0-1m} / R_{1-13}$ x 100% (6)

Where R_{1-13} is the total rainfall amount from the P1 to P13 rainfall processes. Additionally, we compared the averaged SM profile and total soil water storage variation (SWS_{total}) for the 6 months among the study sites:

$SWS_{total} = \sum_{i=1}^{5} AVM_i \times D_i \times 10$ (7)

where AVM_i represents the absolute variation in SM across the entire monitoring period at layer i.

2.2.5 Statistical analysis

The Kruskal–Wallis test was used to test the differences in RT, response duration time, and WFV among different rainfall patterns and vegetation types, in which data were not normally distributed. The Bonferroni method was used to correct pairwise comparisons ($\alpha=0.05$). A one-way analysis of variance was conducted to compare the difference in soil water storage over the growing season. Least significant difference (LSD) was used as a post hoc-test for multiple comparisons of means ($\alpha=0.05$). Linear regression models were established between the total rainfall amount and the change in soil water storage in the 13th rainfall-soil wetting process. Statistical analyses were conducted using the SPSS statistical package (SPSS 22.0, SPSS Inc., Chicago, USA) and Origin 9.3 (OriginLab, Corp., Northampton, MA, USA).

3. RESULTS

3.1 Rainfall characteristics and soil moisture dynamics

5

During the study period from May 1 to October 31, the precipitation instrument recorded 1-h rainfall and accumulated rainfall. The total rainfall reached 565.3 mm, accounting for 94.5% of the annual rainfall amount in 2019. A total of 13 rainfall events are described in Fig. 2f and Table 2, including the total amount, duration, and intensity, which were divided into four groups. Group I (P1 and P3) represented the heavy rainfall that was characterized by a relatively large amount and high peak intensity of rainfall. Group II (P2 and P4) represented intermediate rains with a short duration and high average intensity. Group III (P5, P6, P7, P12, and P13) represented light rains characterized by a short duration and low peak intensity. Group IV (P8, P9, P10, and P11) represented continuous rains with a long duration and a low intensity (Table 2).

Fig. 2 shows that the SM was positively correlated with rainfall input but fluctuated in different levels of different soil layers after precipitation. The results indicated that distinct cycles of wetting and drying in response to rainfall were evident in the shallow soil layer (10 and 30 cm soil depths). However, the deeper layers (70 and 100 cm soil depths) showed a gentle fluctuation range, which was confined in response to rainfall (Fig. 2).

3.2 Soil moisture response depth to rainfall

Different rainfall patterns with different rainfall inputs significantly impacted the soil moisture response depth across the five experimental sites. Total amounts larger than 15.2 mm, 22.2 mm, and 114.2 mm could trigger SM responses at depths of 10, 30, and 70 cm, respectively. For example, heavy rains (Group I) infiltrated to a soil depth of at least 70 cm, while intermediate rains were limited at the 30 cm depth (Fig. 3). In addition, rainfall duration and intensity had a similar impact on the soil wetting depth. When the rainfall duration was greater than 2.3 h, 13.0 h, and 22.0 h, the rainwater could percolate to soil depths greater than 10, 30, and 70 cm, respectively. An average rainfall intensity larger than 0.6 mm/h, 1.3 mm/h, and 6.2 mm/h could stimulate SM responses at depths of 10, 30, and 70 cm, respectively (Fig. 3).

Land cover also strongly influenced the soil wetting depth after precipitation. The average response depth was as follows: grass (57.5 cm) > forest (52.5 cm) > bare land (49.7 cm) > shrub (46.2 cm) > crop (45.4 cm). After converting crops to forests, shrubs, and grasses, the average soil wetting depth increased by 15.7%, 1.7%, and 26.7%, respectively (Supplemental Fig. S1). Two heavy rains (P1 and P3) are obvious, which permitted rainwater to enter deeper soil in forest and grass sites than in other sites (Fig. 3). In intermediate rains (P2 and P4), vegetation recovery prevented rainfall infiltration, leading to a lighter SM response or nonresponse after rainfall (Fig. 3a, c-e). However, the SM of planted shrubs and bare land responded more deeply than that of the other sites (Fig. 3b, e). For light rains and continuous rains, forest and grass sites had deeper soil wetting depths in some specific response processes, such as at P6 and P10.

3.3 Soil moisture response time at the 10-cm soil depth

The SM response exhibited a hysteresis effect after rainfall, and the average response lag time (ART) was 5.6 h at a depth of 10 cm for all precipitation events. Group IV (continuous rains) showed the most obvious hysteresis effect ($p < 0.05$) in which the ART reached 7.8 h, followed by Group III (light rains), Group I (heavy rains), and Group II (intermediate rains) in Table 3. In addition, the l0 cm SM response duration showed a similar trend after precipitation, followed by Group IV (21.9 h) > Group III (14.7 h) > Group II (13.4 h) > Group I (9.7 h). Therefore, a small rainfall amount with a lower intensity significantly delayed the surface SM response time and duration, while a higher rainfall intensity promoted a quick surface SM response.

Land-cover change significantly influenced the surface SM response time ($p < 0.05$). Abandoned grass and planted forest showed a longer ART of 10 cm SM that surpassed 8 h, which was delayed 69.8% and 56.6%, respectively, compared to the crop type. While the shrub site was the exception and showed the earliest ART of surface SM, merely 3.4 h (Table 3 and Supplemental Fig. S2). The lasting response time of the 10-cm SM showed no significant difference among the five vegetation types (Table 3).

In addition, the minimum ARA necessary to trigger the SM response was approximately the same (5-5.9

6

mm) at all the monitoring sites (Fig. 4). The shrub site required the smallest ARA, approximately 5 mm, to trigger a 10-cm SM response, whereas the other sites required ~6 mm (the green dashed line in Fig. 4). The median value of the ARA needed to trigger the SM response was the lowest at the shrub site and highest at the forest site (the red line of the box plot in Fig. 4).

3.4 Soil moisture response velocity to rainfall

Two rainfall process was selected (P1 and P9) to clarify the percolation process of rainfall (Table 4 and Fig. 5). Through the analysis of different rainfall patterns, we found that Group IV has the longest RT and the slowest wetting front velocity (WFV, cm/h) within the 1-m profile. Group II had the shortest RT, approximately 6.4 h, which was significantly lower than that of the other patterns (p<0.05). Group I had the slowest WFV of 10 cm but the fastest WFV in the 1-m profile, which surpassed 6 cm/h (Table 4).

The effect of land-cover change showed that the crop site had the longest RT and slowest WFV in the 1-m profile at a nonsignificant level across the five monitoring sites (Table 4). Nevertheless, revegetation patterns altered this condition, with a smaller RT and a larger WFV. Specifically, planted shrubs accelerated the WFV by approximately 46.7% of the surface SM and reduced the RT by approximately 33.7% across the entire profile compared to the crops. Abandoned grass and planted forest improved the soil permeability to decrease the ART by approximately 17.4% and 30.8%, respectively, and increased the WFV by approximately 87.0% and 77.9%, respectively, in the 1-m profile compared to the crops (Supplemental Fig. S3). Hence, revegetation sites decreased the RT and accelerated the WFV to a great degree.

3.5 Soil water storage over the soil wetting process and growing season

Regression analysis showed that the P1 to P13 rainfall processes ($R_{1\text{-}13}$) and the change in soil water storage along the 1-m profile ($SWS_{0\text{-}1 \text{ m}}$) had a highly positive linear correlation at the 0.05 significance level under all land-cover types (Fig. 5a). The regression model of planted forest exhibited the highest slope value, approaching 0.78, followed by grass, bare land, shrub, and crop sites (Fig. 5a). Similarly, planted forest had the largest increment in $SWS_{0\text{-}1 \text{ m}}$ (217.0 mm) and the highest rainfall transformation rate (RTR), approximately 45% (Fig. 5b). The crop site showed the smallest $SWS_{0\text{-}1 \text{ m}}$ (129.3 mm) and RTR (26.8%). Moreover, our results indicated that revegetation improved rainwater interception, which increased the $SWS_{0\text{-}1\text{m}}$ by approximately 67.7%, 6.1%, and 31.9% for planted forest, shrub, and abandoned grass, respectively, compared to cropland, which promoted soil water infiltration and soil water storage (Fig. 5b).

The SM dynamic and SWS variation over the growing season showed that the average soil water content (ASWC) first increased and then decreased with increasing soil depth (Fig. 6). The ASWC of the grass site (16%) was significantly higher than that of the other sites across the entire profile (p<0.05), followed by forest (11.6%), shrub (9.5%), bare land (9.4%), and crop (8.1%). Moreover, land cover changed the distribution of the ASWC along the 1-m profile over the growing season. For the bare land and crop sites, the lowest ASWC occurred at the 0-10 cm depth, while the highest occurred at the 10-30 cm depth. After planting forest/grass and shrub, the highest ASWC occurred at the 70 cm and 50 cm soil depths over the growing season (Fig. 6), which was beneficial to the deep SM sustainability and vegetation growth supply.

A significant difference between the change in soil water storage (SWS_{total}) among the five monitoring sites over the growing season was discovered (p<0.05). The forest site had the largest SWS_{total} relative to the initial condition, approaching 83.3 mm. This was followed by the crop, grass, and shrub, all with approximately 60 mm increments of SWS_{total}, which were not significantly different. The bare land had the minimum increment over the growing season, merely 46.5 mm (Fig. 6). The above results illustrated that land cover significantly changed the infiltration pattern and SWS_{total}. In Fig. 6, the average SWS_{total} variation in revegetation construction (forest, shrub, and grass), approximately 68.1 mm, was higher than that of crop and bare land in the 0-1 m soil profile (p<0.05). This is the crucial implication that vegetation construction and recovery contributed to water storage and conservation within the 1-m profile in the growing season.

4. DISCUSSION

NOTE: The manuscript illustrates the response and utilization of soil moisture to rainfall under different land covers. Currently, the relationship between artificial vegetation and soil moisture comes to the critical stage, which is not only related to depletion and utilization of soil water, but also soil hydrological processes and sustainability. How to maximum use limited rainfall to replenish soil moisture and optimize vegetation types is of great guiding significance for vegetation construction, especially in arid and semiarid regions of the world.

4.1 Effect of rainfall on soil moisture dynamics

In the Chinese Loess Plateau (CLP), precipitation is the main source of soil moisture (SM) (Jia et al., 2017; Su and Shangguan, 2019). Although the average annual precipitation decreased over nearly half a century on the CLP (Fu et al., 2017), the season-rainstorm occurrence frequency did not significantly change with vegetation construction (Tang et al., 2018). However, under rainstorms, the runoff (Lü et al., 2012) and sediment (Wang et al., 2016) concentrations decreased significantly after afforestation, such as the "Grain For Green Project", radically altering the rainfall-SM response relationship, which intercepts rainfall, delays surface runoff, and increases rainwater infiltration (Kijowska-Strugala et al., 2018). Nevertheless, the characteristics of the soil water cycle process have changed, and the extent and process of this change are still unclear.

Our results concluded that the rainfall-SM response exhibited a positive but not synchronous correlation. The fluctuation of SM occurred after precipitation, especially in larger amounts of rainfall. The shallow soil layers were more susceptible to rainfall than deep layers (Fig. 2). This phenomenon was more obvious under different rainfall patterns with different rainfall amounts, durations, and intensities in the CLP (Hou et al., 2018; Jin et al., 2018; Tang et al., 2019). For example, heavy rains (Group I) with a larger amount and intensity had the deepest SM response depth, at least 70 cm depth (Fig. 3), which was similar to Wang et al. (2013). Tang et al. (2019) also illustrated that a larger rainfall amount could promote rainwater percolation into deeper soil. However, high intensity with a continuous input of rainfall might surpass the max-rate of soil permeability and limit the soil water infiltration in the shallow layer (Yan et al., 2021), resulting in the shortest lasting time of the 10-cm depth and the slowest permeating velocity of the 100-cm profile (Tables 3 and 4). Compared with heavy rains, intermediate rains (Group II) showed the shallowest response depth (Fig. 3) but the shortest response time (RT) of the entire profile and the fastest wetting front velocity (WFV) of the 10-cm SM (Tables 3 and 4). It was indicated that small rains with a high rainfall intensity could penetrate the dense canopy cover and litter layer to trigger a surface SM response in the most effective way of all the rainfall patterns, which was similar to the results of Liu et al. (2020). Continuous rains (Group IV) were the most lagging and slowest pattern to cause an SM feedback. For instance, continuous rains not only lagged in RT of the entire depth but also showed the smallest WFV in the 1-m profile across all rainfall patterns. This result was mainly due to a smaller rainfall amount with a longer duration stretching the rainfall time and decreasing the average rainfall intensity, which made it difficult to through the canopy and litter layer, and to store rainwater in the surface soil layer. There has not been enough water to trigger the SM response and infiltrate into the deep layer at a larger speed of the soil wetting front, due to the lack of guidance from the gravitational water potential (Mao et al., 2018). Therefore, a high average rainfall intensity with a smaller rainfall amount promotes a quick surface SM response, but a larger rainfall amount facilitates rainwater percolation into deeper soil with a larger WFV.

In addition, regardless of the vegetation pattern, the surface SM (10-cm depth) responded only when the minimum accumulated rainfall amount (ARA) surpassed 5 mm. This conclusion is slightly different from Jin et al. (2018), who demonstrated that a 9 mm ARA was necessary to trigger surface SM variation. Perhaps the difference in canopy coverage and litter depth due to vegetation age, which revegetation after 60 years in Jin et al. (2018). After 20 years of revegetation in this region, a 5 mm ARA was the threshold needed to replenish soil water, which was consumed by plant-inducing dried soil layers (Jia et al., 2017; Wang et al., 2011). It is suggested that the constraint of a minimum ARA exists in terms of vegetation restoration in semiarid CLP.

4.2 Effect of land cover on the soil wetting process

In the case of a certain rainfall amount, land-cover type was the key factor that determined the SM response. Different land-cover patterns have different vegetation structures, coverage (canopy, herb, litter), root depths and densities, and soil textures, which influence the soil wetting process after precipitation (Chen et al., 2007a; Jia et al., 2017; Li and Shao, 2006; Zhang et al., 2021).

First, the rainfall-SM average response depth increased by 15.7%, 1.7%, and 26.7% when the crop was transformed to forest, shrub, and grass sites, respectively (Supplemental Fig. S1). Vegetation recovery altered the plant coverage and structure radically, resulting in changes in the way and process of soil acceptance from precipitation (Lozano-Parra et al., 2015; Wang et al., 2013). Specifically, planted forests, with a higher canopy and greater litter coverage, intercepted the large rainfall and weakened the dynamic potential energy of heavy rains in large amounts. One part of the rainfall is intercepted by the canopy and flows down the trunk to the soil directly, and the part of rainfall may reach the litter layer as throughfall. The thick and rough litter hampered the formation of surface runoff and percolated rainwater infiltration to the deep soil layer. This vegetation structure promoted an SM response deeper in planted forests after heavy rains (Fig. 3a). Abandoned grass improved soil texture, decreased soil bulk density, and increased soil porosity, which was also beneficial for rainfall-SM infiltration (Sun et al., 2018). Especially in Fig. 3c, permitting percolation to the 100 cm depth occurred in heavy rains. Planted shrubs with a high coverage could not reach the deepest monitoring layer, probably due to SM consumption by root absorption and vegetation evapotranspiration (Yu et al., 2017). Additionally, the shrub site showed a shallower average wetting depth than that of bare land across the 13 rainfall events (Supplemental Fig. S1). This is because smaller rainfall amounts with short durations have difficulty penetrating dense canopies and thick litter layers of shrubs to percolate into subsurface soil (Wang et al., 2013). Compared to afforestation covers, bare land had a deeper average soil wetting depth than shrub and crop sites after precipitation. Because no vegetation coverage results in direct rainfall and surface soil cracks that increased soil water percolation access together promoted rainwater infiltration into a deeper layer in bare land. These results suggested that land cover strongly influenced the rainfall-SM response depth, while revegetation promoted rainwater percolation to deeper depths across the profile.

Second, the rainfall-surface SM response lag time (RT) and lasting time changed significantly due to land-cover change. The results showed that shrub has the smallest RT and lasting time at the 10-cm depth (Table 3 and Fig. 4). This case was correlated to the initial SM that influenced the speed of rainwater infiltration (Liu et al., 2019). Due to excessive soil water consumption by vast evapotranspiration (including soil and plants) and deeper root water absorption, the shrubland showed the smallest SM across the entire profile, especially in the surface layer. The extremely dry situation accelerated soil water permeation, which was demonstrated by Li et al. (2015) and Sun et al. (2018), who illustrated that a lower initial soil water content accelerated the topsoil permeability rate. Thus, planted shrubs have the shortest response and duration. Compared to shrubs, planted forests and abandoned grass show longer RT and shorter durations. Due to the existence of a dense canopy and a thick litter layer, rainfall is blocked to a large extent and postpones the contact time of rainfall-SM, resulting in a longer response. Meanwhile, much infiltrated rainwater percolates into deep soil or counterbalanced with plant consumption, also decreasing the SM duration at the 10-cm depth. Thus, the effect of afforestation on the surface SM response time or duration after rainfall was significantly different. However, with no vegetation coverage, bare land showed a smaller RT and the longest duration. Because bare land does not have vegetation shade or litter cover, rainwater directly contacts the surface soil and decreases the SM feedback time. Therefore, vegetation recovery delays the surface SM response time but shortens the duration after precipitation, except for shrubs.

Finally, the change in land-cover type influenced the SM response time and wetting front velocity (WFV). For example, the crop site required more time to respond to rainfall, resulting in the longest ART and the slowest WFV across the entire profile. Vegetation restoration altered this situation. Vegetation restoration no only shortened the ART by approximately 30.8%, 33.7%, and 17.4% but also accelerated the WFV by approximately 77.9%, 36.7%, and 87.0% for planted forest, shrub, and grass, respectively, over the 1-m depth (Table 4 and Supplemental Fig. S3). This difference in soil permeability was related to soil texture. Afforestation improved soil texture, decreased soil bulk density and increased soil porosity, which facilitated

9

rainwater percolation across the profile (Sun et al., 2018). Thus, revegetation had the shorter RT and higher WFV, which benifited for alleviating the soil water deficit caused by plant water consumption.

In conclusion, vegetation restoration has a significant impact on ecohydrological processes, including rainfall-SM response depth, RT, and WFV. Despite afforestation consuming more soil water and causing soil desiccation to a large extent. However, the rainfall-SM response process showed that revegetation (mean value of forest, shrub, and grass) increased the soil wetting depth by 14.7%, shortened the ART by 27.3%, and accelerated the WFV by 67.2% compared to cropland over the entire profile. Revegetation contributed to rainwater infiltration and deeper SM replenishment in the rainy season.

4.3 Effect of revegetation on the 'soil reservoir'

On the CLP, the thick loess has a very high water storage capacity, which can accumulate all the natural rainfall and regulate the balance of soil water to sustain plant growth. Vegetation recovery and sustainable development are mainly dependent on the level of SM and the stock amount of the 'soil reservoir'. Many previous studies have shown that SM and SWS decrease significantly after revegetation, causing a temporary or permanent dry soil layer (Jia et al., 2017; Su and Shangguan, 2019). This desiccation situation of the soil profile limits the replenishment of soil water after precipitation. In turn, the lack of the supply capacity of the soil reservoir further restricts plant growth, such as the 'old-man small tree' (Wang et al., 2010a; Wang et al., 2010b). For example, Zeng et al. (2017) and Chai et al. (2019) demonstrated that after planting for 30 yrs, leguminous shrubs (*C. korshins*) will decrease the soil quality and continuously reduce the SM, resulting in premature decay and death. Nevertheless, not all vegetation recovery types exhibit functional degradation and recession. The main reason for this situation is whether the soil water of the soil reservoir can maintain sustainable vegetation growth. In particular, it is important to note whether the soil water that is consumed by the plants in the dry season can be replenished by rainfall in the rainy season. Therefore, we researched the changes in the SM and SWS of each land-cover type after rainfall events and over the whole plant growing season.

We concluded that land-cover change, especially vegetation recovery, had a significant impact on soil water accumulation and utilization after rainfall (Fig. 5). In our study, revegetation remodeled the interrelation between SM and rainfall. Letting the plants act as the intermediate medium and forming a relatively continuous and discontinuous unity, the roots of plants dig deep into the soil but block rainfall from coming into direct contact with the soil. These changes in plant structure and function of land cover promoted much more rainwater percolating into the 'soil reservoir', which increased the SWS by approximately 67.7%, 6.1%, and 31.9% in the planted forest, shrub, and grass, respectively, compared to the cropland over the 13 rainfall events (Fig. 5). The reason is that forest and grass sites with a higher canopy coverage and a thick litter layers hamper precipitation to a large extent, reducing the erosion of surface soil and increasing the retention of rainwater (Jian et al., 2015), especially for heavy rains. When the amount of rainfall surpasses the interception capacity of vegetation, rainwater will reach the soil. At this moment, the continuum that the roots of plants related to soil begin to play their roles. The dense fine roots form a multi-porous structure and establish a multipath water infiltration channel, promoting rainwater infiltration into deeper soil with a short response time. For example, the abandoned grass exhibited preferential flow in the subsurface soil layer after continuous rains (Fig. 5h). In addition, the improvement of soil properties by vegetation, which decreased the bulk density and increased the SOC, all increased the infiltration rate of soil water. The final result is that the forest site had the largest response value of slope correlation (Fig. 5a) and the largest change in the SWS at the 0-1 m soil depth after all the soil wetting processes, followed by grass (Fig. 5b). Nevertheless, planted shrubs with similar characteristics of revegetation did not store more soil water after precipitation, mainly because plant absorption and evapotranspiration exacerbated the entire soil water depletion profile. The accumulated amount after precipitation was not enough to compensate for vegetation water consumption. The shrub site had the shortest RT and fastest WFV in the surface soil but was not helpful for alleviating soil desiccation and increasing soil water accumulation. This result suggested that planted shrubs may not be suitable for this limited rainfall region on the semiarid CLP, especially after 20 years of revegetation. We also concluded that the rainfall-SM response pattern determined the utilization

10

and storage patterns of soil water of different land-cover types. The deeper the response depth was, the shorter the response time was, and the higher the velocity of subsurface soil was, the larger the increment of SWS and rainfall utilization rate (RUR) in rainfall processes.

Further study illustrated that the seasonal SM distribution and SWS changed significantly across the five monitoring sites over the growing season. Revegetation improved the average soil water content (ASWC) across the profile, with a higher RUR and infiltration amount, despite planted shrubs depleting much more soil water. Meanwhile, planting trees and grass, instead of cultivation or bare land, promoted rainwater reaching deeper soil, which showed that the largest ASWC value occurred at deeper depths after revegetation (Fig. 6). This result was due to soil permeability promotion, particularly in subsurface profiles, which accelerated the speed of soil water infiltration and responded in the deeper layer. Additionally, due to the higher canopy coverage and thick litter layer of woodland (Jian et al., 2015) and lower evapotranspiration of grass (Wang et al., 2012), which depleted less water from deeper soils in the growing season, the soil water of the revegetation type could sustain a higher content in deep soil. For SWS variation over the growing season (SWS_{total}), planted forest had the largest increment in SWS_{total}, which was significantly higher than that at the other sites. The utilization and conservation pattern of forests resulted in greater SWS_{total} accumulation. For example, a deeper soil wetting depth for infiltration (Fig. 3), a faster WFV of the subsoil layer (Table 4), a higher utilization rate (RUR) of rainfall (Fig. 5b), and the roughest surface cover intercepted rainwater and runoff. The consumption and conservation pattern also confined the condition of SWS_{total}. For example, shrubs with vigorous evapotranspiration in the growing season depleted a considerable amount of water in the 1-m profile, causing severe soil desiccation (Wang et al., 2011) that was counterbalanced with infiltrated rainwater. This result was limited to storing much more water in the profile over the rainy season. However, the grass site was the opposite. With less aboveground biomass and evapotranspiration, the grass site possessed the lowest soil water consumption and the highest soil water content before the rainy season. However, the higher initial SM of abandoned grass limited the range of change in the SWS if the soil was saturated with water that was not very dry (Su et al., 2019). Thus, planted shrub and abandoned grass sites showed smaller amplitude variations in the SWS_{total} than did forests and even crop sites over the growing season (Fig. 6). Unlike revegetation with high canopy recovery and thick litter to intercept rainfall and increase infiltration, bare land with no vegetation cover mostly exacerbated the soil erosion of the soil surface caused by heavy rainfall, which limited the percolation of water to deep soils. Moreover, the direct solar radiation intensified the evaporation of the entire soil profile. Together, these factors led to the smallest increase in the SWS of bare land across the five monitoring sites over the growing season (Fig. 6e). Therefore, revegetation types did not aggravate the water deficit of the 0-1 m soil depth after precipitation in the growing season. In turn, the existence of vegetation promoted rainwater infiltration into deeper soil layers, which is beneficial to the SWS increase in 'soil reservoir and plant sustainable development'. This paper concentrated on the rainfall-SM response process of 20-year revegetation types over the growing season only, while further research should be conducted on the interaction between plants and soil water at a longer temporal, a larger spatial, and deeper profile scales on the CLP.

5. CONCLUSIONS

This paper conducted hly soil moisture monitoring of the plant growth season on the CLP and found that the constraint of the minimum accumulated rainfall amount stimulated the surface soil moisture response. A minimum rainfall amount of 5 mm was required to trigger a soil moisture response at a depth of 10 cm at the shrub site, while the other sites demanded ~6 mm. With a larger rainfall amount and higher intensity, rainwater can infiltrate deeper and faster along the 1-m soil profile. Across all the land-cover types, revegetation sites, especially forest and grass, had a deeper response depth, shorter response time, faster response velocity, higher rainfall transformation rate and higher soil water storage of all the rainfall processes in the 1-m profile. These results suggested that rainfall patterns, land-cover types, and their interplays together determined the soil moisture response process. Moreover, after 20 years of vegetation reconstruction, land-cover change can regulate the rainfall-soil moisture response relationship (soil moisture response depth, time, and velocity) and promote rainfall resource utilization efficiency (rainfall transformation rate and soil water storage), which does not aggravate the soil water deficit across the 1-m profile over the rainy season.

11

Therefore, while considering the joint effect of precipitation and land-cover change on soil moisture and soil water storage, abandoned grass may be the best choice for sustainable plant–soil water utilization when the rainfall amount is less than 550 mm, while planted forest, instead of shrub, is beneficial for rainfall utilization and ecosystem water conservation if precipitation is greater than 550 mm.

ACKNOWLEDGEMENTS

REFERENCES

Bryan, B. A., Gao, L., Ye, Y. Q., Sun, X. F., Connor, J. D., Crossman, N. D., Stafford-Smith, M., Wu, J. G., He, C. Y., Yu, D. Y., Liu, Z. F., Li, A., Huang, Q. X., Ren, H., Deng, X. Z., Zheng, H., Niu, J. M., Han, G. D., Hou, X. Y., 2018. China's response to a national land-system sustainability emergency. Nature 559 (7713), 193-204. https://doi.org/10.1038/s41586-018-0280-2.

Chai, Q., Ma, Z., An, Q., Wu, G.-L., Chang, X., Zheng, J., Wang, G., 2019. Does Caragana korshinskii plantation increase soil carbon continuously in a water-limited landscape on the Loess Plateau, China? Land Degrad. Dev. 30 (14), 1691-1698. https://doi.org/10.1002/ldr.3373.

Chen, L., Huang, Z., Gong, J., Fu, B., Huang, Y., 2007a. The effect of land cover/vegetation on soil water dynamic in the hilly area of the loess plateau, China. Catena 70 (2), 200-208. https://doi.org/10.1016/j.catena.2006.08.007.

Chen, L., Wei, W., Fu, B., Lu, Y., 2007b. Soil and water conservation on the Loess Plateau in China: review and perspective. Prog. Phys. Geogr. 31 (4), 389-403. https://doi.org/10.1177/0309133307081290.

Chirino, E., Bonet, A., Bellot, J., Sanchez, J. R., 2006. Effects of 30-year-old Aleppo pine plantations on runoff, soil erosion, and plant diversity in a semi-arid landscape in south eastern Spain. Catena 65 (1), 19-29. https://doi.org/10.1016/j.catena.2005.09.003.

Deng, L., Shangguan, Z. P., 2017. Afforestation Drives Soil Carbon and Nitrogen Changes in China. Land Degrad. Dev. 28 (1), 151-165. https://doi.org/10.1002/ldr.2537.

Ding, W., Wang, F., Dong, Y., Jin, K., Cong, C., Han, J., Ge, W., 2021. Effects of rainwater harvesting system on soil moisture in rain-fed orchards on the Chinese Loess Plateau. Agric. Water Manag. 243, 106496. https://doi.org/10.1016/j.agwat.2020.106496.

Birdsey, R., Pan, Y., 2015. Trends in management of the world's forests and impacts on carbon stocks. For. Ecol. Manag. 355: 83-90. http://dx.doi.org/10.1016/j.foreco.2015.04.031.

Feng, S., Fu, Q., 2013. Expansion of global drylands under a warming climate. Atmos. Chem. Phys. 13 (19), 10081-10094. https://doi.org/10.5194/acp-13-10081-2013.

Fu, B., Wang, S., Liu, Y., Liu, J., Liang, W., Miao, C., 2017. Hydrogeomorphic Ecosystem Responses to Natural and Anthropogenic Changes in the Loess Plateau of China. In: Jeanloz, R., Freeman, K. H., editor, Annual Review of Earth and Planetary Sciences, Vol 45. Annual Review of Earth and Planetary Sciences, p. 223-243. https://doi.org/10.1146/annurev-earth-063016-020552

Hardie, M., Lisson, S., Doyle, R., Cotching, W., 2013. Determining the frequency, depth and velocity of preferential flow by high frequency soil moisture monitoring. J. Contam. Hydrol. 144 (1), 66-77. https://doi.org/10.1016/j.jconhyd.2012.10.008.

He, Z., Jia, G., Liu, Z., Zhang, Z., Yu, X., Hao, P., 2020. Field studies on the influence of rainfall intensity, vegetation cover and slope length on soil moisture infiltration on typical watersheds of the Loess Plateau, China. Hydrol Process 34 (25), 4904-4919. https://doi.org/10.1002/hyp.13892.

He, Z., Zhao, W., Liu, H., Chang, X., 2012. The response of soil moisture to rainfall event size in sub-alpine grassland and meadows in a semi-arid mountain range: A case study in northwestern China's Qilian Mountains. J. Hydrol. 420-421, 183-190. https://doi.org/10.1016/j.jhydrol.2011.11.056.

Hou, G., Bi, H., Wei, X., Kong, L., Wang, N., Zhou, Q., 2018. Response of Soil Moisture to Single-Rainfall Events under Three Vegetation Types in the Gully Region of the Loess Plateau. Sustainability 10 (10), 3793. https://doi.org/10.3390/su10103793.

Huang, J., Yu, H., Guan, X., Wang, G., Guo, R., 2016. Accelerated dryland expansion under climate change. Nat. Clim. Chang. 6 (2), 166-171. https://doi.org/10.1038/nclimate2837.

Jia, X., Shao, M. A., Zhu, Y., Luo, Y., 2017. Soil moisture decline due to afforestation across the Loess Plateau, China. J. Hydrol. 546, 113-122. https://doi.org/10.1016/j.jhydrol.2017.01.011.

Jia, Y.-H., Shao, M. A., 2014. Dynamics of deep soil moisture in response to vegetational restoration on the Loess Plateau of China. J. Hydrol. 519, 523-531. https://doi.org/10.1016/j.jhydrol.2014.07.043.

Jian, S., Zhao, C., Fang, S., Yu, K., 2015. Effects of different vegetation restoration on soil water storage and water balance in the Chinese Loess Plateau. Agric. For. Meteorol. 206, 85-96. https://doi.org/10.1016/j.agrformet.2015.03.009.

Jin, Z., Guo, L., Lin, H., Wang, Y., Yu, Y., Chu, G., Zhang, J., 2018. Soil moisture response to rainfall on the Chinese Loess Plateau after a long-term vegetation rehabilitation. Hydrol Process 32 (12), 1738-1754. https://doi.org/10.1002/hyp.13143.

Koutroulis, A. G., 2019. Dryland changes under different levels of global warming. Sci. Total Environ. 655, 482-511. https://doi.org/10.1016/j.scitotenv.2018.11.215.

Lee, E., Kim, S., 2017. Pattern similarity based soil moisture analysis for three seasons on a steep hillslope. J. Hydrol. 551, 484-494. https://doi.org/10.1016/j.jhydrol.2017.06.028.

Li, B., Li, P., Zhang, W., Ji, J., Liu, G., Xu, M., 2021a. Deep soil moisture limits the sustainable vegetation restoration in arid and semi-arid Loess Plateau. Geoderma 399, 115122. https://doi.org/10.1016/j.geoderma.2021.115122.

Li, B., Zhang, W., Li, S., Wang, J., Liu, G., Xu, M., 2021b. Severe depletion of available deep soil water induced by revegetation on the arid and semiarid Loess Plateau. For. Ecol. Manage. 491, 119156. https://doi.org/10.1016/j.foreco.2021.119156.

Li, Q., Zhu, Q., Zheng, J., Liao, K., Yang, G., 2015. Soil moisture response to rainfall in forestland and vegetable plot in Taihu Lake Basin, China. Chin Geogr Sci 25 (4), 426-437. https://doi.org/10.1007/s11769-014-0715-0.

Li, Y. Y., Shao, M. A., 2006. Change of soil physical properties under long-term natural vegetation restoration in the Loess Plateau of China. J. Arid Environ. 64 (1), 77-96. https://doi.org/10.1016/j.jaridenv.2005.04.005.

Lickley, M., Solomon, S., 2018. Drivers, timing and some impacts of global aridity change. Environ. Res. Lett. 13 (10), 104010. https://doi.org/10.1088/1748-9326/aae013.

Lin, H., Zhou, X., 2008. Evidence of subsurface preferential flow using soil hydrologic monitoring in the Shale Hills catchment. Eur J Soil Sci 59 (1), 34-49. https://doi.org/10.1111/j.1365-2389.2007.00988.x.

Liu, M., Wang, Q., Guo, L., Yi, J., Lin, H., Zhu, Q., Fan, B., Zhang, H., 2020. Influence of canopy and topographic position on soil moisture response to rainfall in a hilly catchment of Three Gorges Reservoir Area, China. J. Geogr. Sci. 30 (6), 949-968. https://doi.org/10.1007/s11442-020-1764-1.

Liu, Y., Miao, H.-T., Huang, Z., Cui, Z., He, H., Zheng, J., Han, F., Chang, X., Wu, G.-L., 2018. Soil water depletion patterns of artificial forest species and ages on the Loess Plateau (China). For. Ecol. Manage.

417, 137-143. https://doi.org/10.1016/j.foreco.2018.03.005.

Liu, Y., Cui, Z., Lopez-Vicente, M., Wu, G.-L., 2019. Influence of soil moisture and plant roots on the soil infiltration capacity at different stages in arid grasslands of china - sciencedirect. Catena 182, 104147-104147. https://doi.org/10.1016/j.catena.2019.104147

Lozano-Parra, J., Schnabel, S., Ceballos-Barbancho, A., 2015. The role of vegetation covers on soil wetting processes at rainfall event scale in scattered tree woodland of Mediterranean climate. J. Hydrol. 529, 951-961. https://doi.org/10.1016/j.jhydrol.2015.09.018.

Lu, Y., Fu, B., Feng, X., Zeng, Y., Liu, Y., Chang, R., Sun, G., Wu, B., 2012. A Policy-Driven Large Scale Ecological Restoration: Quantifying Ecosystem Services Changes in the Loess Plateau of China. PloS One 7 (2), e31782. https://doi.org/10.1371/journal.pone.0031782.

Mamedov, A. I., Levy, G. J., 2019. Soil erosion-runoff relations on cultivated land: Insights from laboratory studies. Eur J Soil Sci 70 (3), 686-696. https://doi.org/10.1111/ejss.12759.

Mayerhofer, C., Meissl, G., Klebinder, K., Kohl, B., Markart, G., 2017. Comparison of the results of a small-plot and a large-plot rainfall simulator – Effects of land use and land cover on surface runoff in alpine catchments. Catena 156, 184-196. http://dx.doi.org/10.1016/j.catena.2017.04.009

McMillan, H. K., Srinivasan, M. S., 2015. Characteristics and controls of variability in soil moisture and groundwater in a headwater catchment. Hydrol Earth Syst Sci 19 (4), 1767-1786. https://doi.org/10.5194/hess-19-1767-2015.

Murray, S. J., 2014. Trends in 20th century global rainfall interception as simulated by a dynamic global vegetation model: implications for global water resources. Ecohydrology 7 (1), 102-114. https://doi.org/10.1002/eco.1325.

Pan, D., Yang, S., Song, Y., Gao, X., Wu, P., Zhao, X., 2019. The tradeoff between soil erosion protection and water consumption in revegetation: Evaluation of new indicators and influencing factors. Geoderma 347, 32-39. https://doi.org/10.1016/j.geoderma.2019.02.003.

Rosenbaum, U., Huisman, J. A., Weuthen, A., Vereecken, H., Bogena, H. R., 2010. Sensor-to-Sensor Variability of the ECH2O EC-5, TE, and 5TE Sensors in Dielectric Liquids. Vadose Zone J. 9 (1), 181-186. https://doi.org/10.2136/vzj2009.0036.

Salve, R., Sudderth, E. A., St Clair, S. B., Torn, M. S., 2011. Effect of grassland vegetation type on the responses of hydrological processes to seasonal precipitation patterns. J. Hydrol. 410 (1-2), 51-61. https://doi.org/10.1016/j.jhydrol.2011.09.003.

Su, B., Shangguan, Z. P., 2019. Decline in soil moisture due to vegetation restoration on the Loess Plateau of China. Land Degrad. Dev. 30 (3), 290-299. https://doi.org/10.1002/ldr.3223.

Sun, D., Yang, H., Guan, D., Yang, M., Wu, J., Yuan, F., Jin, C., 2018. The effects of land use change on soil infiltration capacity in China: A meta-analysis. Sci. Total Environ. 626, 1394-1401. https://doi.org/10.1016/j.scitotenv.2018.01.104.

Tang, M., Zhao, X., Gao, X., Zhang, C., Wu, P., 2019. Land Use Affects Soil Moisture Response to Dramatic Short-term Rainfall Events in a Hillslope Catchment of the Chinese Loess Plateau. Agron. J. 111 (3), 1506-1515. https://doi.org/10.2134/agronj2018.06.0405.

Tang, X., Miao, C., Xi, Y., Duan, Q., Lei, X., Li, H., 2018. Analysis of precipitation characteristics on the loess plateau between 1965 and 2014, based on high-density gauge observations. Atmos. Res. 213, 264-274. https://doi.org/10.1016/j.atmosres.2018.06.013.

Wang, H., Zhang, G., Li, N., Zhang, B., Yang, H., 2019. Soil erodibility as impacted by vegetation restoration strategies on the Loess Plateau of China. Earth Surf. Process. Landf. 44 (3), 796-807. https://doi.org/10.1002/esp.4531.

14

Wang, S., Fu, B., Gao, G., Liu, Y., Zhou, J., 2013. Responses of soil moisture in different land cover types to rainfall events in a re-vegetation catchment area of the Loess Plateau, China. Catena 101, 122-128. https://doi.org/10.1016/j.catena.2012.10.006.

Wang, S., Fu, B., Gao, G., Yao, X., Zhou, J., 2012. Soil moisture and evapotranspiration of different land cover types in the Loess Plateau, China. Hydrol Earth Syst Sci 16 (8), 2883-2892. https://doi.org/10.5194/hess-16-2883-2012.

Wang, S., Fu, B., Piao, S., Lu, Y., Ciais, P., Feng, X., 2016. Reduced sediment transport in the Yellow River due to anthropogenic changes. Nat. Geosci. 9 (1), 38-+. https://doi.org/10.1038/NGEO2602.

Wang, Y., Dong, Y., Su, Z., Mudd, S. M., Zheng, Q., Hu, G., 2020. Spatial distribution of water and wind erosion and their influence on the soil quality at the agropastoral ecotone of North China. Int. Soil Water Conserv. Res. 8 (3), 253-265. https://doi.org/10.1016/j.iswcr.2020.05.001.

Wang, Y., Shao, M. A., Liu, Z., 2010a. Large-scale spatial variability of dried soil layers and related factors across the entire Loess Plateau of China. Geoderma 159 (1-2), 99-108. https://doi.org/10.1016/j.geoderma.2010.07.001.

Wang, Y., Shao, M. A., Shao, H., 2010b. A preliminary investigation of the dynamic characteristics of dried soil layers on the Loess Plateau of China. J. Hydrol 381 (1-2), 9-17. https://doi.org/10.1016/j.jhydrol.2009.09.042.

Wang, Y., Shao, M. A., Zhu, Y., Liu, Z., 2011. Impacts of land use and plant characteristics on dried soil layers in different climatic regions on the Loess Plateau of China. Agric. For. Meteorol. 151 (4), 437-448. https://doi.org/10.1016/j.agrformet.2010.11.016.

Williams, A. P., Cook, E. R., Smerdon, J. E., Cook, B. I., Abatzoglou, J. T., Bolles, K., Baek, S. H., Badger, A. M., Livneh, B., 2020. Large contribution from anthropogenic warming to an emerging North American megadrought. Science 368 (6488), 314-+. https://doi.org/10.1126/science.aaz9600.

Wu, G.-L., Cui, Z., Huang, Z., 2021. Contribution of root decay process on soil infiltration capacity and soil water replenishment of planted forestland in semi-arid regions. Geoderma 404, 115289. https://doi.org/10.1016/j.geoderma.2021.115289.

Yan, W., Zhou, Q., Peng, D., Wei, X., Tang, X., Yuan, E., 2021. Soil moisture responses under different vegetation types to winter rainfall events in a humid karst region. Environ. Sci. Pollut. Res. 28 (40), 56984-56995. https://doi.org/10.1007/s11356-021-14620-z.

Yu, X., Huang, Y., Li, E., Li, X., Guo, W., 2017. Effects of vegetation types on soil water dynamics during vegetation restoration in the Mu Us Sandy Land, northwestern China. J. Arid Land 9 (2), 188-199. https://doi.org/10.1007/s40333-017-0054-y.

Yu, Y., Wei, W., Chen, L., Jia, F., Yang, L., Zhang, H., Feng, T., 2015. Responses of vertical soil moisture to rainfall pulses and land uses in a typical loess hilly area, China. Solid Earth 6 (2), 595-608. https://doi.org/10.5194/se-6-595-2015.

Zeng, Q., Lal, R., Chen, Y., An, S., 2017. Soil, Leaf and Root Ecological Stoichiometry of Caragana korshinskii on the Loess Plateau of China in Relation to Plantation Age. PloS One 12 (1), e0168890. https://doi.org/10.1371/journal.pone.0168890.

Mao, W., Yang, J., Zhu, Y., Ye, M., Liu, Z., Wu, J., 2018. An efficient soil water balance model based on hybrid numerical and statistical methods. J. Hydrol 559, 721-735. https://doi.org/10.1016/j.jhydrol.2018.02.074.

Zhang, Z.-H., Peng, H.-Y., Kong, Y., 2021. Effects of the "Grain for Green" Program on Soil Water Dynamics in the Semi-Arid Grassland of Inner Mongolia, China. Water 13 (15), 2034. https://doi.org/10.3390/w13152034.

Zhao, G., Mu, X., Jiao, J., An, Z., Klik, A., Wang, F., Jiao, F., Yue, X., Gao, P., Sun, W., 2017. Evidence and cause of spatiotemporal changes in runoff and sediment yield on the Chinese Loess Plateau. Land Degrad. Dev. 28 (2), 579-590. https://doi.org/10.1002/ldr.2534.

Zhao, G., Mu, X., Wen, Z., Wang, F., Gao, P., 2013. Soil erosion, conservation, and eco-environment changes in the Loess Plateau of China. Land Degrad. Dev. 24 (5), 499-510. https://doi.org/10.1002/ldr.2246.

Zheng, H., Wang, Y., Chen, Y., Zhao, T., 2016. Effects of large-scale afforestation project on the ecosystem water balance in humid areas: An example for southern China. Ecol. Eng. 89 103-108. https://doi.org/10.1016/j.ecoleng.2016.01.013.

Zhu, P., Zhang, G., Wang, H., Zhang, B., Liu, Y., 2021. Soil moisture variations in response to precipitation properties and plant communities on steep gully slope on the Loess Plateau. Agric. Water Manag. 256, 107086. https://doi.org/10.1016/j.agwat.2021.107086.

Table 1 Basic characteristics of the monitoring sites

Land-cover type	Land-cover type	Year (yr)	Elevation (m)	Slope (°)	Aspect	Position	Canopy Coverage (%)	Herb Coverag (%)
Forest	25	1258	25	East	Middle	74.8	41.0	86.8
Shrub	28	1284	24	Northwest	Bottom	40.0	59.4	71.7
Grass	25	1309	23	Northwest	Middle	-	60.5	44.2
Crop	-	1312	25	Northwest	Middle	-	71.2	40.5
Bareland	-	1295	25	Northwest	Middle	-	-	-

Table 2 Characteristic of rainfall-soil wetting process (P1 to P13) during May to October

Rainfall process	Data	Group no.[a]	Total amount (mm)	Duration (hr)	Duration (hr)	Peak intensity (mm/h)
P1	Jul 22	I	135.9	22.0	75.6	75.6
P2	Jul 10	II	15.2	2.3	75.0	75.0
P3	Aug 3	I	114.2	15.7	44.4	44.4
P4	Oct 12	II	5.9	0.7	37.2	37.2
P5	Jul 20	III	24.7	12.0	25.8	25.8
P6	Aug 26	III	16.6	13.0	25.2	25.2
P7	Jun 22	III	16.1	9.7	24.0	24.0
P8	Oct 15	IV	32.6	23.4	13.8	13.8
P9	Oct 6	IV	26.1	20.4	12.6	12.6
P10	Aug 24	IV	22.2	39.0	10.2	10.2
P11	Jun 27	IV	33.1	17.4	8.4	8.4
P12	Aug 20	III	16.6	7.0	6.6	6.6
P13	Sep 19	III	20.9	8.3	5.4	5.4

[a] The soil wetting events are divided into four groups according to rainfall attributes.

[b] Average intensity is the total rainfall amount divided by duration during soil wetting process.

Table 3 Response lag time and lasting time of different patterns at 10-cm depth

Pattern	Group	N	Response Lag Time (hr) M±SE	Response Lag Time (hr) Min	Response Lag Time (hr) Max	Response Lasting Time (hr) M±SE	Response Lasting Time (hr) Min	Response Lasting Time (hr) Max
Rainfall pattern	Group I	10	6.1±0.4 b	3.5	7.7	9.7±0.6 a	8	13
	Group II	9	2.0±0.3 a	1.1	3.1	13.4±3.4 ab	2	31
	Group III	24	6.4±1.5 b	1.4	34.2	14.7±2.5 a	2	50
	Group IV	20	7.8±1.0 b	2.5	17.6	21.9±2.7 b	8	55
Vegetation pattern	Forest	12	8.3±1.8 B	2.1	24.2	16.1±3.2 A	3	38
	Shrub	13	3.4±0.6 A	1.1	7.6	13.5±2.6 A	2	35
	Grass	12	9.0±2.7 AB	1.9	34.2	14.8±3.0 A	5	40
	Crop	13	5.3±0.9 AB	1.1	12.6	17.6±3.7 A	6	55
	Bareland	13	5.3±0.8 AB	2.0	11.6	17.9±3.9 A	2	50

Note. N: number; M: mean; SE: standard error. The small letter and upper letter represent the significant difference in rainfall patterns and vegetation patterns respectively (p<0.05).

Table 4 SM response time and wetting front velocity of different patterns at 1-m profile

Pattern	Group	N	RT (hr) 0-100 cm M±SE	RT (hr) 0-100 cm Min	RT (hr) 0-100 cm Max	WFV (cm/hr) 0-100 cm M±SE	WFV (cm/hr) 0-100 cm Min	WFV (cm/hr) 0-100 cm Max	N	WFV (cm/hr) 0-10 cm M±SE
Rainfall pattern	Group I	45	20.3±3.3b	3.5	127.5	6.1±1.3b	0.3	40.0	10	1.7±0.1a
	Group II	12	6.4±3.3a	1.1	42.1	5.1±0.8b	0.7	9.5	9	6.0±0.9b
	Group III	53	11.6±1.3ab	1.4	41.4	4.0±0.5b	0.3	20.0	24	2.8±0.4a
	Group IV	68	30.8±3.3c	2.5	117.0	2.0±0.3a	-5.0	10.0	20	1.8±0.2a
Vegetation pattern	Forest	35	18.3±3.0A	2.1	98.0	4.8±1.1 A	0.4	30.0	12	1.9±0.4A
	Shrub	35	17.6±3.0A	1.1	84.0	3.7±0.6 A	0.7	15.0	13	4.2±0.8B
	Grass	38	21.9±3.5A	2.0	86.0	5.1±1.3 A	-5.0	40.0	12	2.1±0.5AB
	Crop	34	26.5±5.5A	1.1	127.5	2.7±0.4 A	0.3	10.0	13	2.9±0.6AB

17

Pattern	Group	RT (hr)	RT (hr)	RT (hr)		WFV (cm/hr)	WFV (cm/hr)	WFV (cm/hr)	WFV (cm/hr)	WFV (cm/hr)	W (
	Bareland 36	19.8±3.5A2.0		90.0		2.9±0.4 A	0.3	10.0	13	2.5±0.4AB	

Note. N: number; M: mean; SE: standard error. The different small letter and upper letter represents the significant difference in rainfall patterns and vegetation patterns respectively (p<0.05).
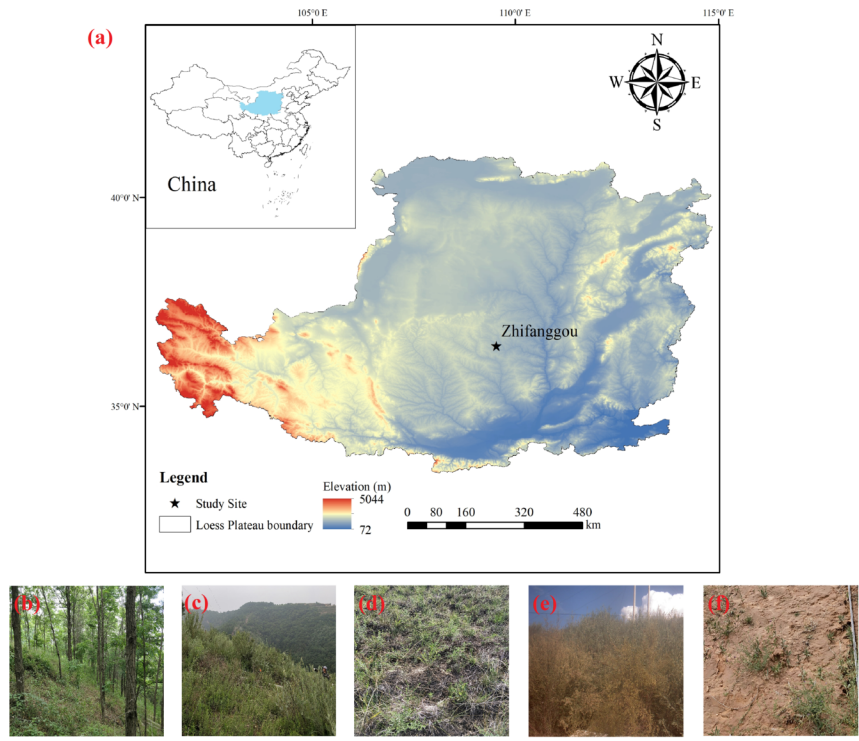
Fig. 1. (a) The study site is located in Zhifanggou watershed of the Chinese Loess Plateau in northern China. (b) Forest site, (c) Shrub site, (d) Grass site, (e) Crop site, and (f) Bareland site.

18
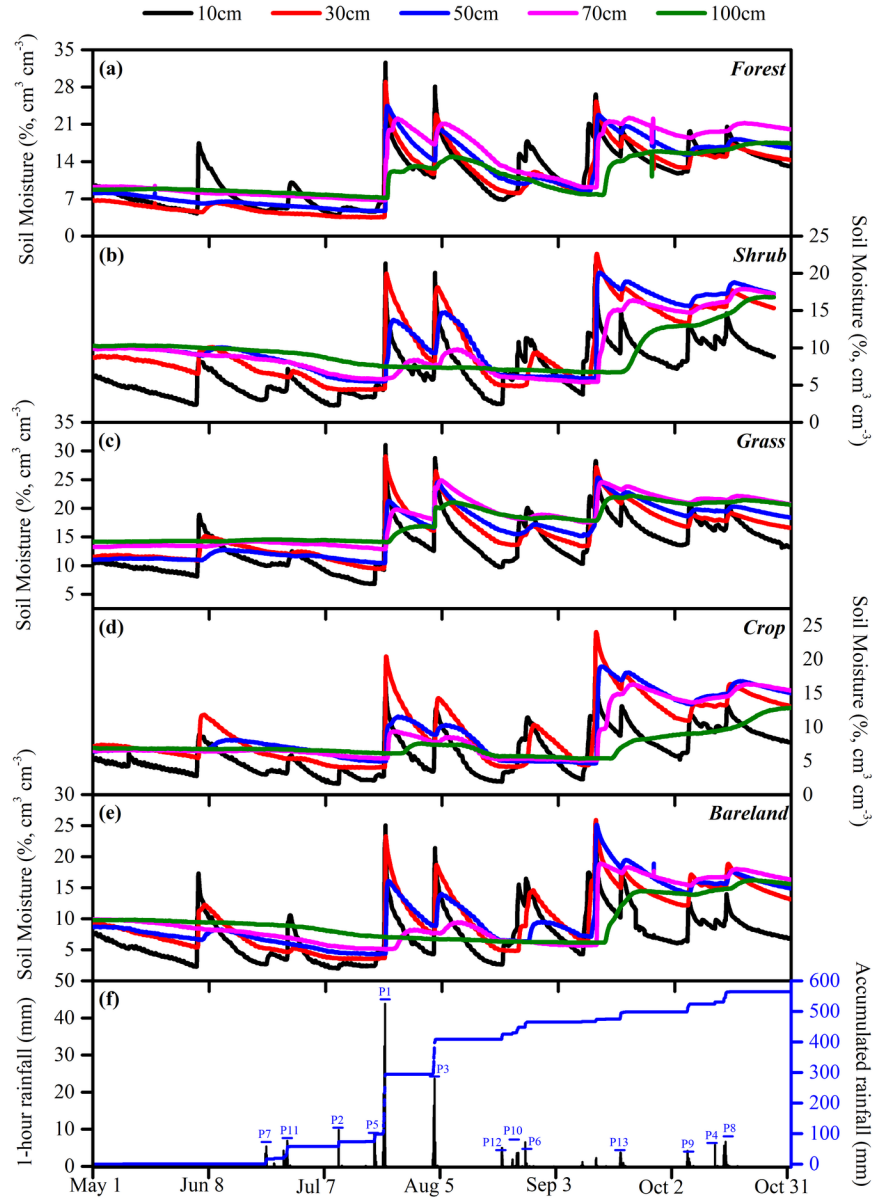
Fig. 2. An overview of 1-hour soil moisture time series and rainfall over the study period (May 1 to October 31, 2019), (a) Forest site, (b) Shrub site, (c) Grass site, (d) Crop site, (e) Bareland site. (f) 1-hour rainfall records over the study period. The blue dashed curve indicates the accumulated rainfall amount over time.
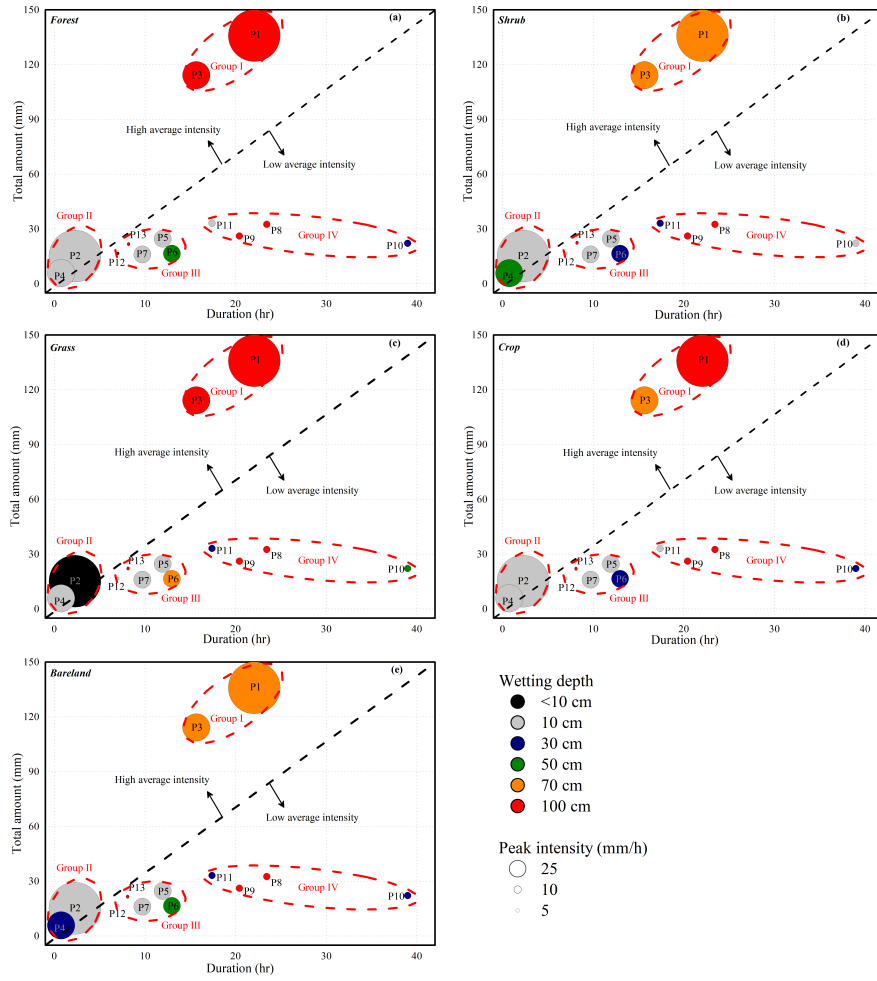
Fig. 3. 13 rainfall-soil wetting processes to soil wetting depth across five monitoring sites. The size of circle represents rainfall peak intensity. The color of each circle indicates different soil wetting depths.

20
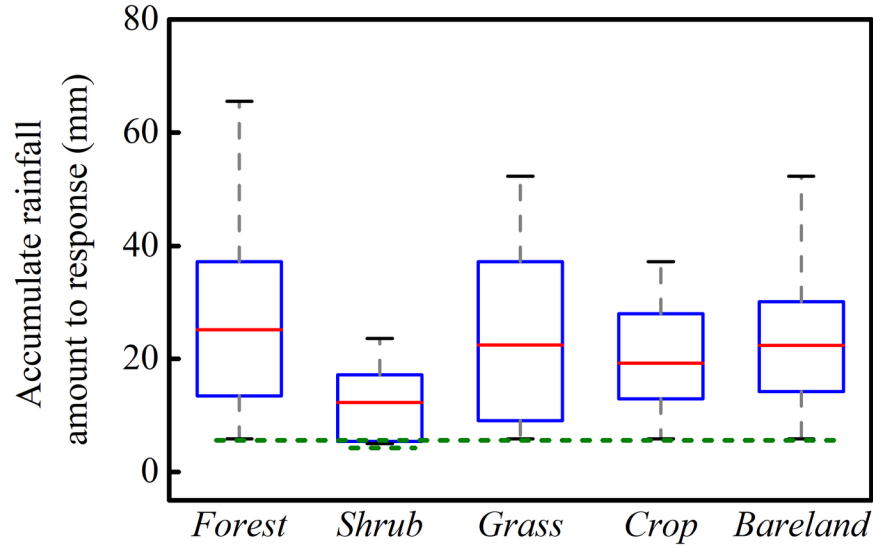
Fig. 4. The accumulated rainfall amount to soil moisture response at the 10-cm depth of all the soil wetting processes across five monitoring sites. The green dashed line represent the threshold accumulated rainfall amount that can trigger 10-cm soil moisture response
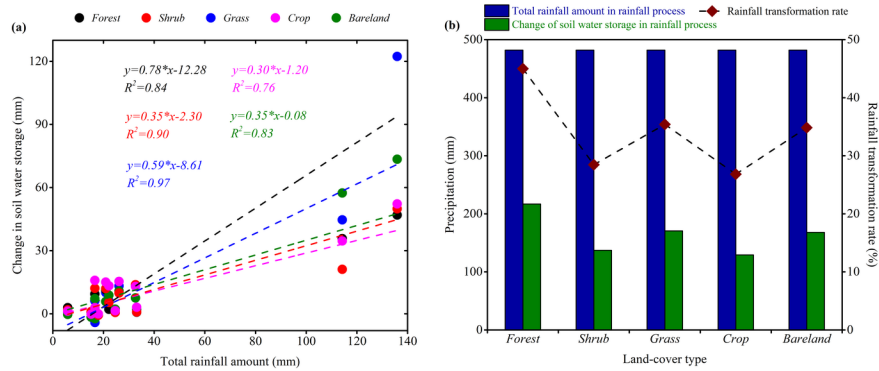

Fig. 5. The relationship between total rainfall amount and the change of soil water storage in the soil wetting process at 0-100 cm soil depth at five monitoring sites. (a): Linear regression analysis between total rainfall amount and the change in soil water storage after each rainfall process. The colored dot represents different land-cover monitoring sites. And dashed lines are the linear regression models, showing the regression equations and coefficients of determination (R^2). (b): Soil water storage variation and rainfall transformation rate at five monitoring sites across all the soil wetting processes. The dashed line with brown diamond icon represents the rainfall transformation rate, which is the ratio of rainwater into the soil.


21
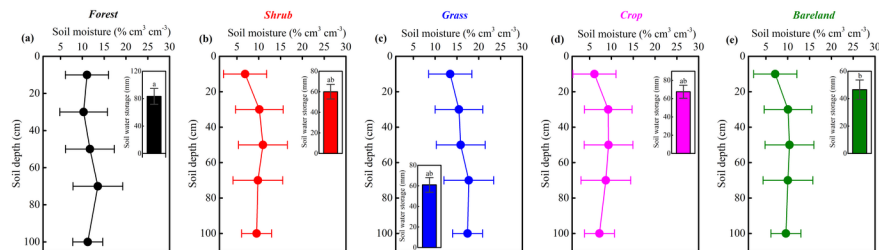
Fig. 6. Soil moisture profile dynamic and soil water storage variation in 0-100 cm soil depth over the growing season. The error bars indicate the standard deviation of the soil moisture and soil water storage among the monitoring sites. The letters on the error bars in the inserted graph is the significant difference in soil water storage across the monitoring sites in probability of 95%.

Supplemental material—Fig. S1
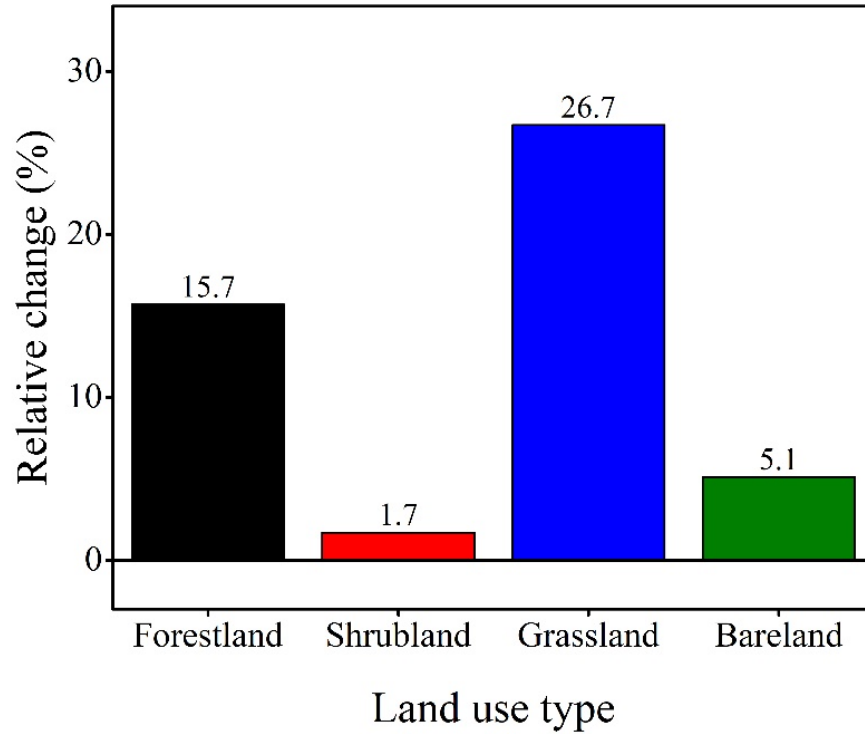
Fig. S1. The relative change of soil wetting depth after rainfall in planted forest, shrub, abandoned grassland, and bareland compared with average cropland soil wetting depth.

Supplemental material—Fig. S2
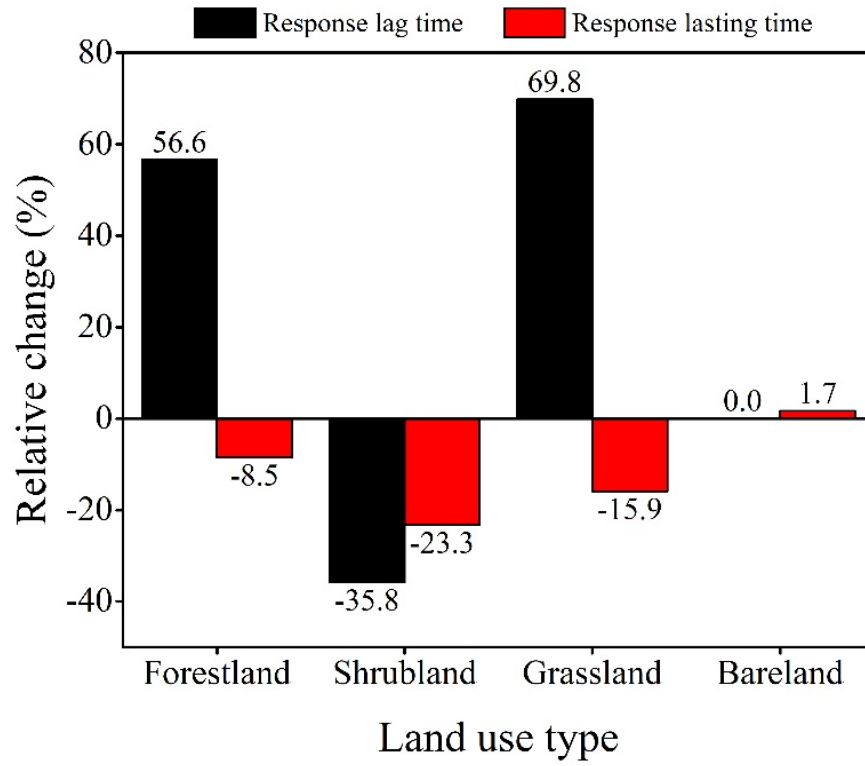
Fig. S2. The relative change of 10-cm soil moisture response lag time and lasting time in planted forest, shrub, abandoned grassland, and bareland compared with average cropland response lag time and lasting time.

Supplemental material—Fig. S3
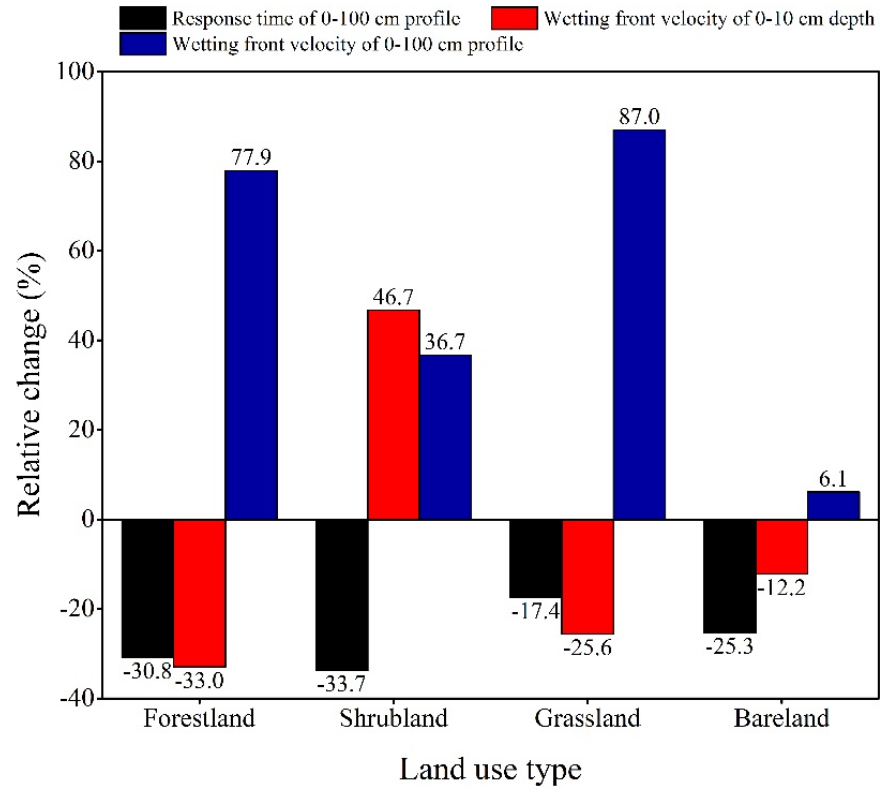
Fig. S3. The relative change of soil moisture response lag time and wetting front velocity in planted forest, shrub, abandoned grassland, and bareland compared with cropland.